IEEE Access
Multidisciplinary : Rapid Review : Open Access Journal

Received October 19, 2018, accepted November 16, 2018, date of publication November 23, 2018,
date of current version December 27, 2018.

Digital Object Identifier 10.1109/ACCESS.2018.2882379

A New Algorithm for Indoor RSSI Radio Map Reconstruction

WEIXING XUE[1,2], QINGQUAN LI[1], XIANGHONG HUA[2], KEGEN YU[3], (Senior Member, IEEE), WEINING QIU[2], AND BAODING ZHOU[1]

[1]Department of Shenzhen Key Laboratory of Spatial Smart Sensing and Services, Shenzhen University, Shenzhen 518060, China
[2]School of Geodesy and Geomatics and the Collaborative Innovation Center for Geospatial Technology, Wuhan University, Wuhan 430079, China
[3]School of Environmental Science and Spatial Informatics, China University of Mining and Technology, Xuzhou 221116, China

Corresponding authors: Qingquan Li (liqq@szu.edu.cn) and Xianghong Hua (xhhua@sgg.whu.edu.cn)

This work was supported in part by the National Key R&D Program of China (2016YFB0502204), in part by National Natural Science Foundation of China under Grant 41674005, Grant 41374011, Grant 91546106, Grant 41701519, Grant 41574031, and Grant 41730109, in part by Natural Science Foundation of Guangdong Province (2017A030310544), and in part by Open Research Fund Program of State Key Laboratory of Information Engineering in Surveying, Mapping, and Remote Sensing (16I02).

ABSTRACT This paper proposes an empirical model of RSSI radio map in order to improve the indoor positioning accuracy of Wi-Fi RSSI. First, the signal feature point in RSSI space is proposed based on the indoor RSSI map, which is similar to the geomorphic feature point in a topographic map. Then, we utilize a small amount of the grid points in geometric space to fill the RSSI grid network by using the theory of low rank matrix. Finally, a new algorithm for indoor RSSI radio map reconstruction has been proposed. Both the grid point in geometric space and the signal feature point in RSSI space have been utilized in the reconstruction of the RSSI empirical model, and different types of feature points have been weighted based on their corresponding positioning accuracy. The proposed algorithm was tested by experiments conducted within a room, and the results indicate that the proposed method significantly outperforms the traditional grid network algorithm.

INDEX TERMS Empirical model, RSSI radio map, the signal feature point, the grid point.

I. INTRODUCTION

Indoor positioning technology has achieved great advances recently mainly due to the rapid advances in information science and technology. Positioning method based on RSSI (Received Signal Strength Indicator) [1]–[3] has become the mainstream for the advantages of low cost, wide coverage and without additional physical hardware [4]–[6]. It is an important aspect of indoor positioning system to establish the location database. There are two categories: the location fingerprint database with collecting the fingerprint reference point RSSI samples in off-line phase, and the forecast database using the propagation model. The location fingerprint database uses a grid network to establish the RSSI database [7]. The forecast RSSI database is established by a propagation model, and this model needs to be trained with RSSI sampling points. In this paper, in order to improve the indoor positioning accuracy of Wi-Fi RSSI, a new algorithm for indoor RSSI radio map reconstruction has been proposed. Similar to the geomorphic feature point in a topographic map, the signal feature point in RSSI space has been proposed for the RSSI radio map reconstruction. The proposed algorithm will be introduced in part II, and the corresponding performance for indoor location is tested in part III.

II. THE PROPOSED ALGORITHM

In order to get a realistically RSSI radio map, both the signal feature point in RSSI space and the grid point in geometric space have been used in the reconstruction of the RSSI empirical model. The signal feature point in RSSI space closely associates with the indoor environment and its internal structure, which can be obtained from a RSSI empirical model. According to [8] and [9], all the grid points in geometric space can be calculated with a small amount of RSSI data by using the low rank matrix theory [10]–[14].

A. RSSI GRID POINTS FILLING WITH LOW RANK MATRIX THEORY

RSSI data on each fingerprint point needs to be sampled in the traditional fingerprint location method, but it is time

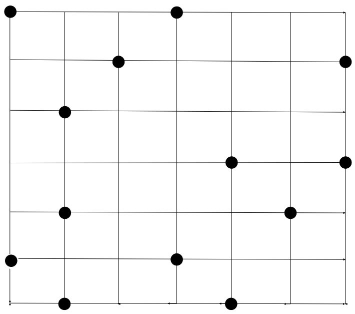

FIGURE 1. The sketch of RSSI sampling.

consuming and manpower consumption. Therefore, compression sensing technology has been proposed [15]–[17]. Compressive sensing provides a new framework for recovering sparse or compressible signals with fewer measurements than that needed by the Nyquist sampling theorem [18], [19].

Low rank matrix filling theory is based on the compression sensing, which mainly solves the problem of how to recover the low rank matrix from sparse measurements [20]. Suppose that the target location area is a rectangular area with $m \times n$ fingerprint points for RSSI data sampling, then every Wi-Fi access point (AP, also termed hotspot) will form a sampling matrix of signal intensity $m \times n$. Assuming that only a small subset of RSSI sampling points is collected, one needs to reconstruct the two-dimensional matrix of the whole target area. The grid points denoted by solid dot are RSSI sampling points, and the rest points need to be filled with low rank matrix theory, as shown in Figure 1.

The target area is defined as matrix $\boldsymbol{X}$, and the number of all grid points is N. In actual sampling, one selects $s\,(s < N)$ grid points for RSSI sampling. The observation matrix denoted as matrix $\boldsymbol{B}$. Therefore, the matrix $\boldsymbol{B}$ is an incomplete matrix with many grid points no-sampling. Then one can establish the relationship between matrix $\boldsymbol{B}$ and matrix $\boldsymbol{X}$, by using the rank minimization theory of the affine matrix, as

$$\begin{aligned} &\min_{X} \ rank(X) \\ &s.t.\, A(X) = B \end{aligned} \tag{1}$$

where $\boldsymbol{A}$ is the linear mapping from the matrix $\boldsymbol{X}$ to the matrix $\boldsymbol{B}$. If one grid point has been sampled, the corresponding RSSI in matrix $\boldsymbol{B}$ is equal to the RSSI of this grid point in matrix $\boldsymbol{X}$. Conversely, if one grid point has not been sampled, then the corresponding RSSI in matrix $\boldsymbol{B}$ is equal to zero. The convex envelope of $rank(X)$ on the set $\{\boldsymbol{X} \in R^{\mathrm{m}\times\mathrm{n}} : \|\boldsymbol{X}\| \leq 1\}$ is the nuclear norm of matrix $\boldsymbol{X}$ [20], as

$$\|X\|_* = \sum_{k=1}^{n} \sigma_k(X) \tag{2}$$

where $\sigma_k(X)$ is the *k-th* singular value matrix $\boldsymbol{X}$. Therefore, by substituting (2) into (1), the combinatorial optimization has been transformed into a convex relaxation optimization, as

$$\begin{aligned} &\min_{X} \ \sum_{k=1}^{n} \sigma_k(X) \\ &s.t.\, A(X) = B \end{aligned} \tag{3}$$

Thus, all elements (RSSI) of matrix $\boldsymbol{B}$ can be filled accurately at a very high probability [20].

Then, one can decompose matrix $\boldsymbol{X}$ by using singular value decomposition as

$$X = U\Sigma V^T \tag{4}$$

where, U is an orthogonal matrix of $m \times m$, Σ is a semi-positive diagonal matrix of $m \times n$, as

$$\Sigma = diag(\sigma_1, \ldots, \sigma_r) \tag{5}$$

V^T is the conjugate transpose matrix of matrix $\boldsymbol{V}$, which is an orthogonal matrix of $n \times n$. Suppose $L = U\Sigma^{1/2}$ and $R = V\Sigma^{1/2}$, by substituting into (1), one can get

$$\begin{aligned} &\min \ rank(LR^T) \\ &s.t.\, A(LR^T) = B \end{aligned} \tag{6}$$

Since there may have multiple solutions of matrix $\boldsymbol{L}$ and matrix $\boldsymbol{R}$, one can optimize them by minimizing the Frobenius norm [21] as

$$\begin{aligned} &\min \|L\|_F^2 + \|R\|_F^2 \\ &s.t.\, A(LR^T) = B \end{aligned} \tag{7}$$

In addition, since the sampling RSSI data may contain errors and the matrix in the location area may not fully be a low rank matrix, the model constraint condition has been transformed into a non-constrained model, as

$$\min \|L\|_F^2 + \|R\|_F^2 + \omega \left\| A(LR^T) - B \right\|_F^2 \tag{8}$$

where ω is the weight matrix of the reconstruction error.

Finally, one can derive the matrix $\boldsymbol{L}$ and $\boldsymbol{R}$ through the alternate iterative process as follows:

1) The least square method has been adopted to calculate the initial value $\boldsymbol{X_0}$ of matrix $\boldsymbol{X}$ and its corresponding possible decomposition matrixes. Then one can select a set of decomposition matrix of matrix $\boldsymbol{X}$ randomly as the initial value of matrix $\boldsymbol{L}$ and matrix $\boldsymbol{R}$.

2) Matrix $\boldsymbol{L}$ is fixed, and matrix $\boldsymbol{R}$ is calculated.

3) Matrix $\boldsymbol{R}$ is fixed, and matrix $\boldsymbol{L}$ is calculated.

4) Repeat step 2, 3 until the target function calculated by formula (8) is convergent.

B. WEIGHT ASSIGNMENT OF NEW NO-OVERLAPPING FILLED GRID POINTS

Once the grid points in geometric space have been filled, there will be overlapping points between the signal feature point in RSSI space and the new filled geometric feature points. For one overlapping point, it has two RSSIs, the sampling RSSI

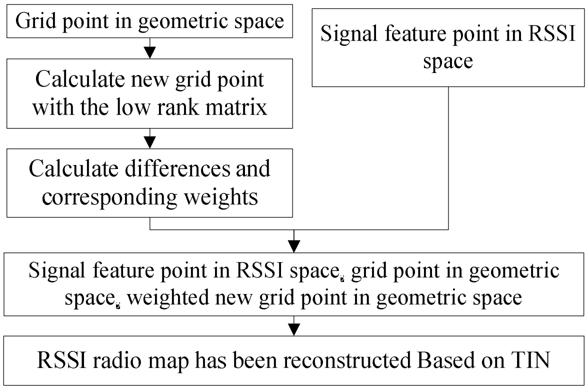

FIGURE 2. **The flowchart of the proposed algorithm.**

and the filled RSSI. Thus, there is a RSSI difference between the sampling RSSI and the filled RSSI, as

$$\Delta RSSI_i = \left| RSSI_i^{sampling} - RSSI_i^{filled} \right| \quad i = 1, 2, \ldots, M \tag{9}$$

where $RSSI_i^{sampling}$ is the sampling RSSI of the i-th overlapping points, $RSSI_i^{filled}$ is the filled RSSI of the i-th overlapping points. It is assumed that there are M overlapping points. The sampling RSSI has been used as its RSSI, while the corresponding RSSI difference has been to assign weights of the no-overlapping filled geometric feature points, by

$$\omega_i' = \frac{1/\Delta RSSI_i}{1\Big/\sqrt{\sum_{i=1}^{M} (\Delta RSSI_i)^2}} \tag{10}$$

After all the weights have been calculated, one can get the Maximum. Taken the Maximum as the reference, weights have been re-calculated as

$$\omega_i' = \frac{\omega_i'}{\omega_{MAX}'} \tag{11}$$

where ω_{MAX}' is the Maximum of all weights.

C. RSSI RADIO MAP RECONSTRUCTION

Finally, the RSSI empirical model is reconstructed by the signal feature points in RSSI space, the grid points in geometric space and the weighted new grid points in geometric space. The method is similar to the way to establish a DEM (Digital Elevation Model), and one can just use RSSI data to replace elevation data. Therefore, the reconstruction of proposed empirical RSSI radio map adopts a fitting model based on the integral interpolation of TIN (Triangular Irregular Network) in [22].

To sum up, the flowchart of the proposed clustering algorithm is shown in Figure 2.

III. EXPERIMENT AND ANALYSIS OF ITS RESULT

In order to evaluate the performance of the proposed algorithm, experiments were conducted in fourth Building of Wuhan University. Figure 3 shows the floor plan of the room 101, where there are 63 points denoted by dot and 6 APs denoted by triangle in the space of 5.2m×3.9m.

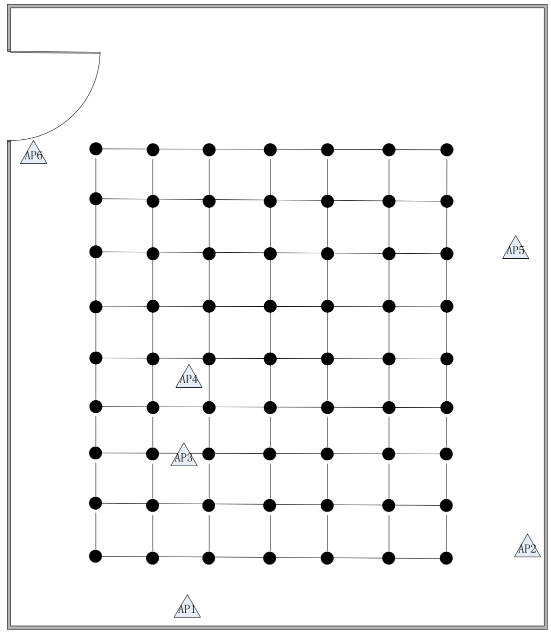

FIGURE 3. **The schematic diagram of experimental point distribution.**

The space of interest in each room is divided into grids whose dimensions are 0.65m×0.65m. The sampling rate of 1 s was used to collect the RSSI. The RSSI data for about five minutes at each point have been used as fingerprint database. To ensure consistency, all the data are collected using the same mobile phone. For convenience, an independent coordinate system in each open area is established for position determination purpose. The grid network of 1.3m×1.3 m has been taken as the fingerprint database of the traditional fingerprint method.

A. RSSI RADIO MAP RECONSTRUCTION WITH THE FEATURE POINTS IN RSSI SPACE

According to the Nyquist sampling theorem [19], the grid network of 0.65m×0.65 m can be taken as the real RSSI radio map of the fingerprint database with network of 1.3m×1.3 m, as shown in Figure 4. For convenience, we take AP1, AP2, AP3 and AP4 as example in all the figures.

From Figure 4, we can see that each of the RSSI radio maps contains mutation points. In other words, there may be coarse error in our sampling data. Therefore, one needs to remove these incorrect sampling points based on the experimental environment firstly. In addition, the incorrect sampling point mainly means the non-boundary point. Since the signal intensity at the boundary is more likely caused by multipath. The elimination of the incorrect sampling points is shown in Table 1.

After removing the incorrect sampling points, the RSSI signal distribution diagram is shown in Figure 5. From Figure 5, we can see that the RSSI radio maps have

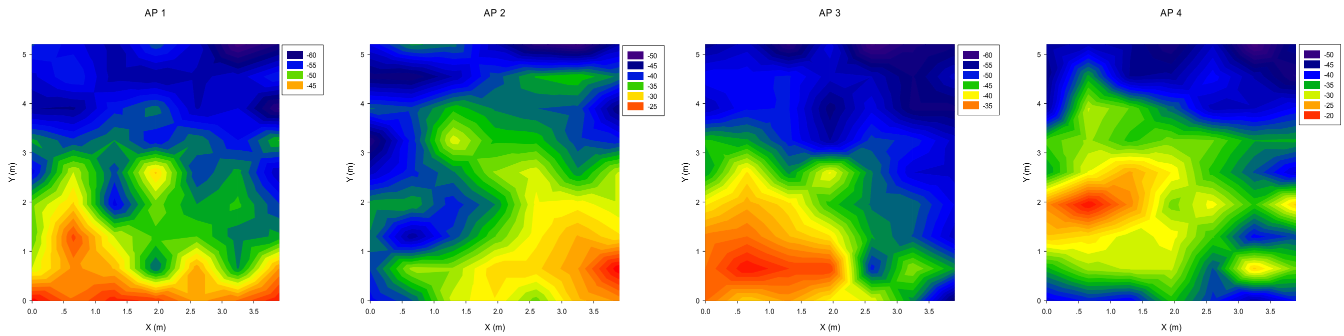

FIGURE 4. The real RSSI radio map.

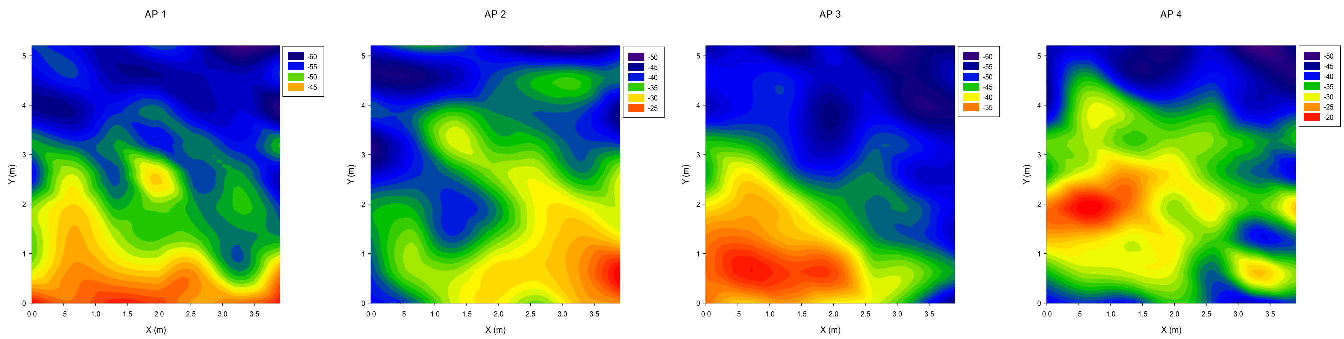

FIGURE 5. The RSSI radio map after removing incorrect sampling points.

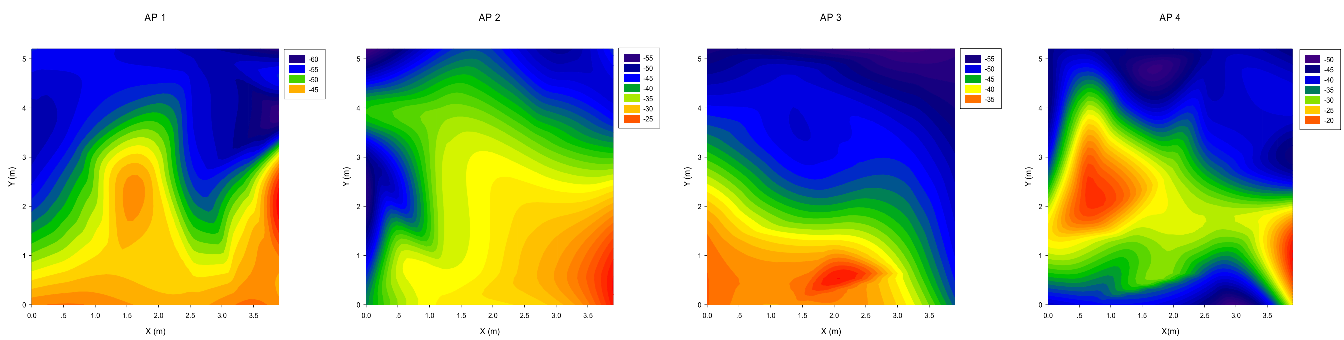

FIGURE 6. Reconstructed RSSI radio map with the feature points in RSSI space.

TABLE 1. The elimination information of different AP.

	AP1	AP2	AP3	AP4	AP5	AP6
Number	3	1	2	1	3	4
Rate (%)	4.76	1.59	3.17	1.59	4.76	6.35

TABLE 2. The feature points selection information of different AP.

	AP1	AP2	AP3	AP4	AP5	AP6
Number	16	19	17	22	17	13
Percentage (%)	25.40	30.16	26.98	34.92	26.98	20.63

been optimized after eliminating the incorrect sampling points. Then, one can select the feature points in RSSI space from Figure 5 according to the corresponding characteristics of each AP RSSI radio map. The number of the feature points in RSSI space may be different from each AP. The number of the feature points in RSSI space and the corresponding percentage of all points are shown in Table 2.

Then, one utilizes these selected feature points to re-construct the RSSI radio map, as shown in Figure 6. From Figure 6, we can see that the RSSI radio map can be outlined roughly with 13∼22 feature points in RSSI space, which is about a quarter of all the grid points in the grid network $0.65\text{m} \times 0.65$ m. Considering that only part of the feature points in RSSI space have been used, the reconstructed RSSI radio map cannot be consistent with the RSSI radio map in Figure 5 completely.

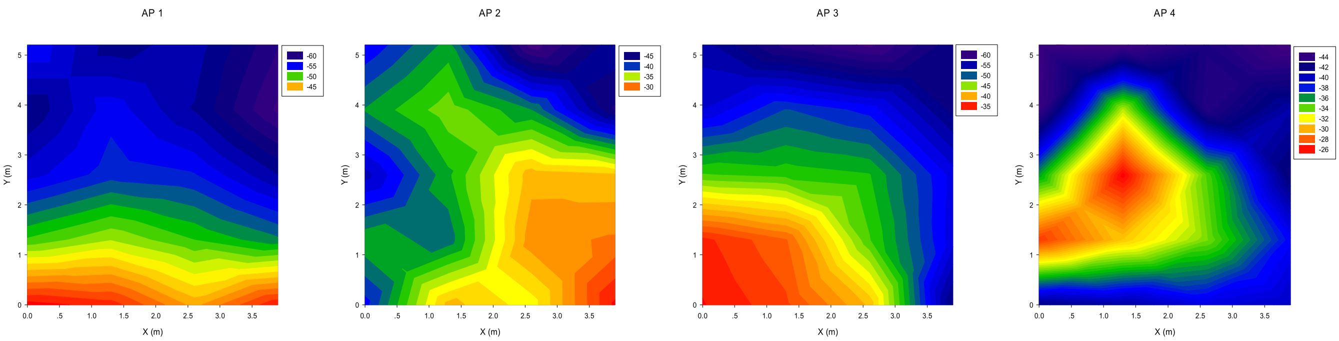

FIGURE 7. Reconstructed RSSI radio map with the grid points in 1.3m×1.3m grid network.

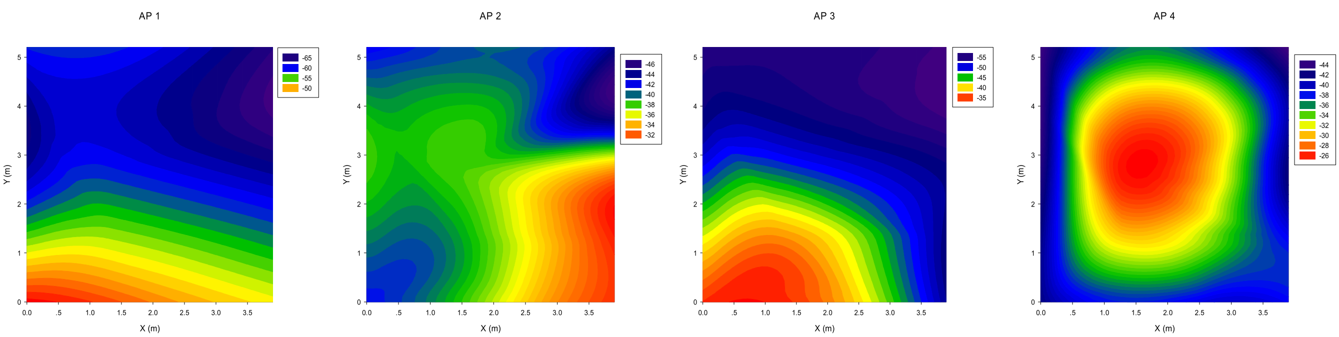

FIGURE 8. Reconstructed RSSI radio map with the sampling grid points.

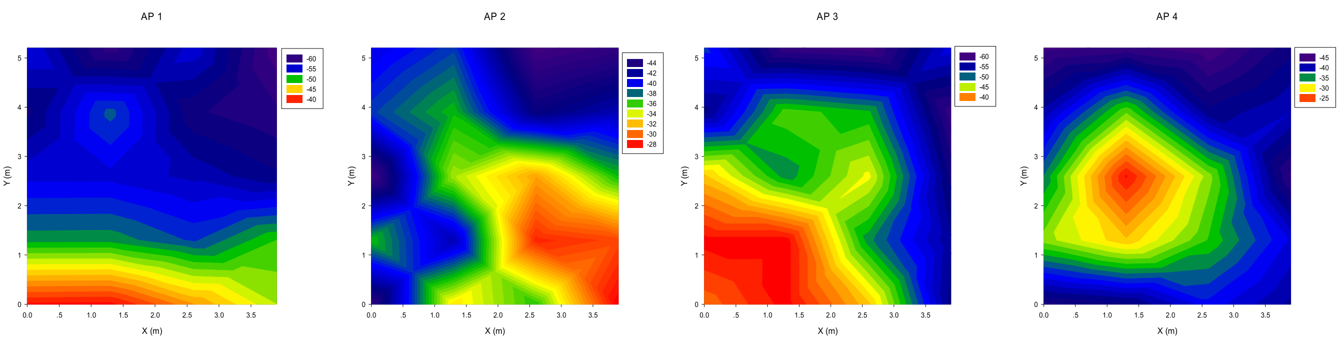

FIGURE 9. Reconstructed RSSI radio map with the theory of low rank matrix filling.

B. RSSI RADIO MAP RECONSTRUCTION WITH THE GRID POINT IN GEOMETRIC SPACE

We use the grid points in 1.3m×1.3m grid network to re-construct the RSSI radio map of the fingerprint, as shown in Figure 7. From the comparison of Figure 7 and Figure 5, it can be seen that the RSSI radio map reconstructed by 1.3m×1.3m grid is roughly the same as the real RSSI radio map. But the detail of this RSSI radio map is not good, which has a large difference with the sampling value of the real RSSI radio map. Therefore, it is not ideal to reconstruct the RSSI radio map only with the grid points in geometric space.

Ten grid points of the sampling RSSI have been randomly chosen from the RSSI radio map of in 1.3m×1.3m grid network, with ensuring that there have sampling RSSI in each row and in each column. Firstly, we use these sampling grid points to re-construct the RSSI radio map, as shown in Figure 8. Then, we re-construct the RSSI radio map by using the low rank matrix filling theory, as shown in Figure 9.

From the comparison of Figure 7 with Figure 9 and Figure 8, it can be seen that similarity between Figure 9 and Figure 7 is greater than similarity between Figure 8 and Figure 7. So the RSSI radio map constructed by the low rank matrix filling theory is better than that that of the selected sampling grid points. In addition, there is a mutation in the RSSI radio map of some AP in Figure 10, which indicates that the RSSI radio map constructed by the low rank matrix filling theory relies on the selected sampling grid points.

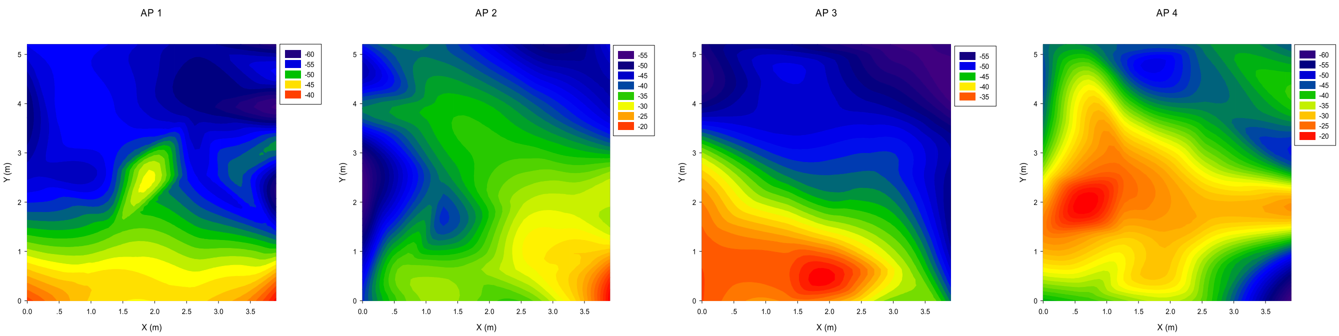

FIGURE 10. The original RSSI radio map with all the feature points.

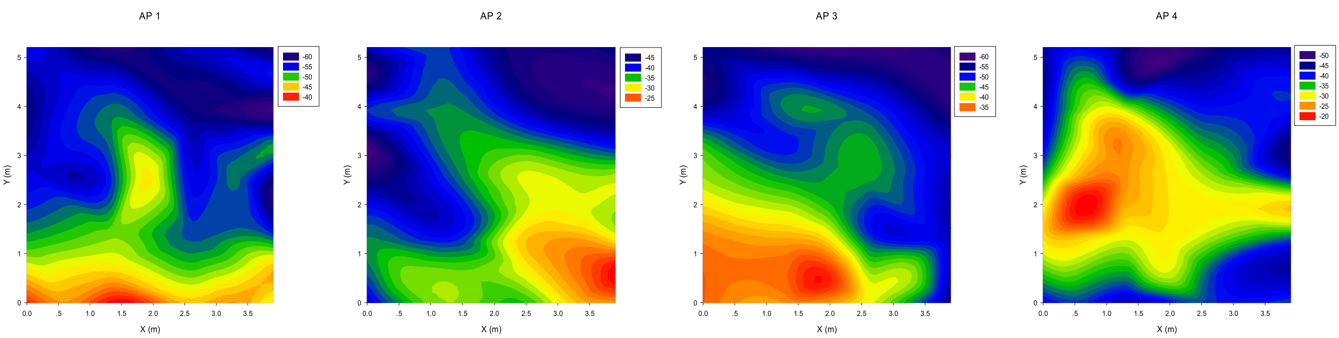

FIGURE 11. The RSSI radio map of the proposed RSSI empirical model.

TABLE 3. Number and proportion of feature points of different AP.

	AP1	AP2	AP3	AP4	AP5	AP6
RSSI points	16	19	17	22	17	13
Grid points	10	10	10	10	10	10
All points	26	29	27	32	27	23
Percentage (%)	41.27	46.03	42.86	50.79	42.86	36.51

Therefore, it is necessary to eliminate the mutation point and to select the sampling grid points randomly.

C. RSSI RADIO MAP RECONSTRUCTION WITH THE PROPOSED ALGORITHM

Table 3 shows the number and proportion of feature points in each AP, and the original RSSI radio map of all the feature points has been re-constructed with all these feature points directly, as shown in Figure 10. Then, the RSSI empirical radio map is reconstructed by combining the signal feature point in RSSI space, the grid point in geometric space and the weighted new grid point in geometric space, as shown in Figure 11.

From the comparison of Figure 5, Figure 7, Figure 10 and Figure 11, we can see that similarity between Figure 11 and Figure 5 is greater than similarity between Figure 10 and Figure 5, and significantly greater than similarity between Figure 7 and Figure 5. Therefore, the positioning accuracy of the RSSI empirical radio map is better than that of the fingerprint algorithm.

TABLE 4. Data sampling information of the two different algorithms.

Algorithm	AP1	AP2	AP3	AP4	AP5	AP6	All
Proposed	26	29	27	32	27	23	164
Fingerprint	20	20	20	20	20	20	120
Workload	1.30	1.45	1.35	1.60	1.35	1.15	1.37

TABLE 5. Positioning accuracy of the two different algorithms.

CDF (%)		0.1(m)	0.2(m)	0.3(m)	0.5(m)	1(m)	2(m)
	AP1	5.00	15.00	25.00	37.50	55.00	82.50
	AP2	7.14	21.43	26.19	45.24	64.29	80.95
	AP3	2.44	14.63	29.27	46.34	73.17	100.00
F	AP4	9.52	16.67	28.57	45.24	69.05	97.62
	AP5	5.00	12.50	25.00	37.50	60.00	77.50
	AP6	10.26	20.51	28.21	43.59	48.72	79.49
	Mean	6.56	16.79	27.04	42.57	61.70	86.34
	AP1	35.00	38.33	46.67	50.00	71.67	91.67
	AP2	38.71	48.39	40.32	62.90	75.81	87.10
	AP3	42.62	47.54	62.30	72.13	88.52	100.00
P	AP4	40.32	45.16	54.84	67.74	82.26	100.00
	AP5	40.00	45.00	48.33	63.33	75.00	91.67
	AP6	35.59	40.68	42.37	47.46	59.32	77.97
	Mean	38.71	44.18	49.14	60.59	75.43	91.40

*Where, F represents the fingerprint algorithm and P represents the proposed algorithm

Next, let us to exam the positioning error of the RSSI empirical radio map. Table 4 shows the RSSI sampling information of the fingerprint algorithm and the RSSI empirical model. There are about 60 RSSI sampling points of each AP after removing several mutations. The positioning error is calculated based on the RSSI differences in meters between the reconstructed RSSI and the real RSSI, as shown in Table 5.

From Table 4 and Table 5, it can be seen that the positioning accuracy of the proposed RSSI empirical model is significantly higher than that of the location fingerprint with a slightly bigger data sampling, especially within 0.5 meter. Therefore, the RSSI empirical model for indoor location does have research meaning and application value.

IV. CONCLUSION

This paper proposed a new algorithm for indoor RSSI radio map reconstruction based on the signal feature point in RSSI space and the low rank matrix filling theory. The signal feature point in RSSI space is first proposed in this paper, which is similar to the geomorphic feature point in a topographic map. The RSSI empirical model is reconstructed by combining the signal feature points in RSSI space, the grid points in geometric space and the weighted new grid points in geometric space. The positioning accuracy of the proposed algorithm was tested by experiments conducted within a room, and the results indicate that the proposed RSSI empirical model significantly outperforms the traditional grid network algorithm.

REFERENCES

[1] X. Tian, R. Shen, D. Liu, Y. Wen, and X. Wang, "Performance analysis of RSS fingerprinting based indoor localization," *IEEE Trans. Mobile Comput.*, vol. 16, no. 10, pp. 2847–2861, Oct. 2017.
[2] W. Xue *et al.*, "A new weighted algorithm based on the uneven spatial resolution of RSSI for indoor localization," *IEEE Access*, vol. 6, pp. 26588–26595, 2018.
[3] W. Xue, K. Yu, X. Hua, Q. Li, W. Qiu, and B. Zhou, "APs' virtual positions-based reference point clustering and physical distance-based weighting for indoor Wi-Fi positioning," *IEEE Internet Things J.*, vol. 5, no. 4, pp. 3031–3042, Aug. 2018.
[4] C. L. Nguyen, O. Georgiou, Y. Yonezawa, and Y. Doi, "The wireless localization matching problem," *IEEE Internet Things J.*, vol. 4, no. 5, pp. 1312–1326, Oct. 2017.
[5] W. Xue, W. Qiu, X. Hua, and K. Yu, "Improved Wi-Fi RSSI measurement for indoor localization," *IEEE Sensors J.*, vol. 17, no. 7, pp. 2224–2230, Apr. 2017.
[6] S. Bi, L. Han, and S. Pan, "Approximation of rank function and its application to the nearest low-rank correlation matrix," *J. Global Optim.*, vol. 57, no. 4, pp. 1113–1137, 2013.
[7] A. Dankar, S. Reddy, M. P. Mortier, M. F. Buhrmann, C. L. Dennis, and R. A. Snyder, "System and method for automated analysis comparing a wireless device location with another geographic location," U.S. Patent 8 374 634, Feb. 12, 2013.
[8] D. L. Donoho, "Compressed sensing," *IEEE Trans. Inf. Theory*, vol. 52, no. 4, pp. 1289–1306, Apr. 2006.
[9] L. Li, and P. Liu, "A survey of the greedy reconstruction algorithm based on gradient in compressed sensing," *J. Nanjing Univ. Posts Telecommun., Natural Sci. Ed.*, vol. 34, no. 6 pp. 1–8, 2014.
[10] C. Guillemot and O. L. Meur, "Image inpainting: Overview and recent advances," *IEEE Signal Process. Mag.*, vol. 31, no. 1, pp. 127–144, Jan. 2014.
[11] E. J. Candès, J. Romberg, and T. Tao, "Robust uncertainty principles: Exact signal reconstruction from highly incomplete frequency information," *IEEE Trans. Inf. Theory*, vol. 52, no. 2, pp. 489–509, Feb. 2006.
[12] X. Zhou and W. Yu, "Low-rank modeling and its applications in medical image analysis," *Proc. SPIE Defense, Secur., Sens.*, vol. 8750, pp.87500V-1–87500V-10, May 2013.
[13] G. Yuan, "Low rank approximation algorithm of matrix and its application," School Comput. Sci. Eng., South China Univ. Technol., Guangzhou, China, Tech. Rep., 2013.
[14] X. Zhou *et al.*, "Low-rank modeling and its applications in image analysis," *Acm Computing Surv.*, vol. 47, no. 2, pp. 1–35, 2015.
[15] E. J. Candès and M. B. Wakin, "An introduction to compressive sampling," *IEEE Signal Process. Mag.*, vol. 25, no. 2, pp. 21–30, Mar. 2008.
[16] J. Romberg, "Imaging via compressive sampling," *IEEE Signal Process. Mag.*, vol. 25, no. 2, pp. 14–20, Mar. 2008.
[17] A. Akl and S. Valaee, "Accelerometer-based gesture recognition via dynamic-time warping, affinity propagation, & compressive sensing," in *Proc. IEEE Int. Conf. Audio Speech Signal Process. (ICASSP)*, Mar. 2010, pp. 2270–2273.
[18] C. Feng, W. S. A. Au, S. Valaee, and Z. Tan, "Received-signal-strength-based indoor positioning using compressive sensing," *IEEE Trans. Mobile Comput.*, vol. 11, no. 2, pp. 1983–1993, Dec. 2012.
[19] C. W. Mccombie, "Nyquist's theorem and its generalisations," in *Problems in Thermodynamics and Statistical Physics*. London, U.K.: Pion Ltd., 1971.
[20] B. Recht, M. Fazel, and P. A. Parrilo, "Guaranteed minimum-rank solutions of linear matrix equations via nuclear norm minimization," *SIAM Rev.*, vol. 52, no. 3, pp. 471–501, 2010.
[21] T. Nakayama, "On Frobeniusean algebras. I," *Ann. Math.*, vol. 40, no. 3, pp. 611–633, 1939.
[22] M. P. Kumler, "An intensive comparison of triangulated irregular networks (TINs) and digital elevation models (DEMs)," *Cartographica, Int. J. Geograph. Inf. Geovis.*, vol. 31, no. 2, pp. 1–99, 1994.

WEIXING XUE was born in Luyi, Henan, China, in 1990. He received the bachelor's degree from the School of Geodesy and Geomatics, Wuhan University, in 2016, where he is currently pursuing the Ph.D. degree. His research interests include seamless positioning and navigation, multi sensor information fusion and data processing theory, and precision engineering measurement.

QINGQUAN LI received the Ph.D. degree in geographic information system (GIS) and photogrammetry from the Wuhan Technical University of Surveying and Mapping, Wuhan, China, in 1998. He is currently a Professor with Shenzhen University, Guangdong, China, and Wuhan University, Wuhan.

His research areas include 3-D and dynamic data modeling in GIS, location-based service, surveying engineering, integration of GIS, Global Positioning System and remote sensing, intelligent transportation system, and road surface checking.

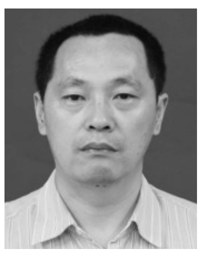

XIANGHONG HUA was born in Taixian, Jiangsu, China, in 1963. He received the Ph.D. degree in engineering from Wuhan University in 2006. He is currently a Professor of geodesy and surveying engineering and the Director of the Hazard Monitoring and Prevention Research Center, Wuhan University.

His research interests include engineering survey and thematic GIS, 3-D laser scanning data processing and quality evaluation, engineering and disaster monitoring and forecasting, multi sensor information fusion, and seamless positioning and navigation technology.

KEGEN YU (SM'12)) received the Ph.D. degree in electrical engineering from The University of Sydney, Sydney, NSW, Australia, in 2003.

He was with the Jiangxi Geological and Mineral Bureau, and later with Nanchang University, Nanchang, China, the University of Oulu, Oulu, Finland, CSIRO ICT Centre, Sydney, Australia, Macquarie University, Sydney, and the University of New South Wales, Sydney. Since 2011, he has been an Adjunct Professor with Macquarie University. He is currently a Professor with the School of Environmental Science and Spatial Informatics, China University of Mining and Technology, Xuzhou, China. He has co-authored the book *Ground-Based Wireless Positioning* (Wiley and IEEE Press)–a Chinese version of the book is also available. He has authored or co-authored over 90 refereed journal and conference papers. His current research interests include global navigation satellite systems (GNSS) reflectometry and ground-based and satellite-based positioning.

Dr. Yu currently serves on the editorial boards of the *EURASIP Journal on Advances in Signal Processing*, the IEEE TRANSACTIONS ON AEROSPACE AND ELECTRONIC SYSTEMS, and the IEEE TRANSACTIONS ON VEHICULAR TECHNOLOGY. He was the Lead Guest Editor for a special issue of *Physical Communication* on Indoor Navigation and Tracking, and for a special issue of the *EURASIP Journal on Advances in Signal Processing* on GNSS Remote Sensing.

WEINING QIU was born in Liangping, Sichuan, China, in 1956. She received the master's degree in engineering from Wuhan University in 1994. After graduating from school, she was promoted to Associate Professor in 1994 and a Professor in 1999 with Wuhan University. From 1996 to 1997, she conducted a cooperative research at The Hong Kong Polytechnic University. She has been involved in the teaching and research in surveying engineering and surveying and mapping data processing for over 30 years.

BAODING ZHOU received the Ph.D. degree in photogrammetry and remote sensing from Wuhan University, Wuhan, China, in 2015. He is currently a Post-Doctoral Fellow with the Shenzhen Key Laboratory of Spatial Smart Sensing and Service, Shenzhen University, Shenzhen, China. His research interests include indoor localization and mapping, mobile computing, and intelligent transportation.